

## Molecular Dynamics at the Root of Expansion of Function in the M69L Inhibitor-Resistant TEM $\beta$ -Lactamase from *Escherichia coli*

Samy O. Meroueh,<sup>†</sup> Pierre Roblin,<sup>‡</sup> Dasantila Golemi,<sup>†</sup> Laurent Maveyraud,<sup>‡</sup>  
Sergei B. Vakulenko,<sup>†</sup> Yun Zhang,<sup>†</sup> Jean-Pierre Samama,<sup>\*‡</sup> and  
Shahriar Mobashery<sup>\*†</sup>

Contribution from the Groupe de Cristallographie Biologique, Institut de Pharmacologie et de Biologie Structurale du CNRS, 205 route de Narbonne, 31077 Toulouse Cedex, France, and Institute for Drug Design and the Department of Chemistry, Wayne State University, Detroit, Michigan 48202-3489

Received April 16, 2002

**Abstract:** Clavulanate, an inhibitor for  $\beta$ -lactamases, was the very first inhibitor for an antibiotic resistance enzyme that found clinical utility in 1985. The clinical use of clavulanate and that of sulbactam and tazobactam, which were introduced to the clinic subsequently, has facilitated evolution of a set of  $\beta$ -lactamases that not only retain their original function as resistance enzymes but also are refractory to inhibition by the inhibitors. This article characterizes the properties of the clinically identified M69L mutant variant of the TEM-1  $\beta$ -lactamase from *Escherichia coli*, an inhibitor-resistant  $\beta$ -lactamase, and compares it to the wild-type enzyme. The enzyme is as active as the wild-type in turnover of typical  $\beta$ -lactam antibiotics. Furthermore, many of the parameters for interactions of the inhibitors with the mutant enzyme are largely unaffected. The significant effect of the inhibitor-resistant trait was a relatively modest elevation of the dissociation constant for the formation of the pre-acylation complex. The high-resolution X-ray crystal structure for the M69L mutant variant revealed essentially no alteration of the three-dimensional structure, both for the protein backbone and for the positions of the side chains of the amino acids. It was surmised that the difference in the two enzymes must reside with the dynamic motions of the two proteins. Molecular dynamics simulations of the mutant and wild-type proteins were carried out for 2 ns each. Dynamic cross-correlated maps revealed the collective motions of the two proteins to be very similar, yet the two proteins did not behave identically. Differences in behavior of the two proteins existed in the regions between residues 145–179 and 155–162. Additional calculations revealed that kinetic effects measured experimentally for the dissociation constant for the pre-acylation complex could be mostly attributed to the electrostatic and van der Waals components of the binding free energy. The effects of the mutation on the behavior of the  $\beta$ -lactamase were subtle, including the differences in the measured dissociation constants that account for the inhibitor-resistant trait. It would appear that nature has selected for incorporation of the most benign alteration in the structure of the wild-type TEM-1  $\beta$ -lactamase that is sufficient to give the inhibitor-resistant trait.

Enzymes evolve to fulfill the biochemical needs of living organisms. The selection pressure drives such evolutionary events, a process that is dynamic and, depending on the life cycle of the given organism, can be quite rapid. Bacterial production of  $\beta$ -lactamases, resistance enzymes that hydrolytically degrade  $\beta$ -lactam antibiotics, has been an effective countermeasure in the face of the extensive use of these antibiotics in the clinic in the past 50 years. Over 340 distinct  $\beta$ -lactamases have been identified,<sup>1,2</sup> a number of which are known to carry out their catalytic reactions at or near the diffusion limit.<sup>3,4</sup>

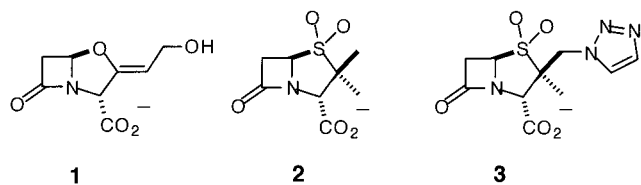
Clavulanate (**1**), a natural product inhibitor for the most prevalent class A  $\beta$ -lactamases, was introduced to the clinic in 1985 in a preparation with penicillin. Clavulanate would inhibit the  $\beta$ -lactamases, whereby the penicillin would inhibit the target penicillin-binding proteins, resulting in bacterial death. This strategy has been extremely successful, and its success led to introduction of two synthetic inhibitors for  $\beta$ -lactamases, sulbactam (**2**) and tazobactam (**3**), in subsequent years.

\* To whom correspondence should be addressed. J.-P.S.: phone (33) 5-61-17-54-44, fax (33) 5-61-17-54-48, E-mail Jean-Pierre.Samama@ipbs.fr. S.M.: phone (313) 577-3924, fax (313) 577-8822, E-mail som@chem.wayne.edu.

<sup>†</sup> Institut de Pharmacologie et de Biologie Structurale du CNRS.

<sup>‡</sup> Wayne State University.

- (1) Kotra, L. P.; Samama, J. P.; Mobashery, S. Structural Aspects of  $\beta$ -Lactamase Evolution. In *Bacterial Resistance to Antimicrobials, Mechanisms, Genetics, Medical Practice and Public Health*; Lewis, A., Salyers, A. A., Haber, H., Wax, R. G., Eds.; Marcel Dekker: New York, 2002; p 123.
- (2) Bush, K.; Mobashery, S. How  $\beta$ -Lactamases Have Driven Pharmaceutical Drug Discovery: from Mechanistic Knowledge to Clinical Circumvention. *Adv. Exp. Med. Biol.* **1998**, 456, 71.
- (3) Bulychiev, A.; Mobashery, S. *Antimicrob. Agents Chemother.* **1999**, 43, 1743.
- (4) Hardy, L. W.; Kirsch, J. F. *Biochemistry* **1984**, 23, 1275.



Clinical availability of these inhibitors for  $\beta$ -lactamases precipitated evolution of a new kind of  $\beta$ -lactamases over the past 16 years, one that remains catalytically competent as a resistance enzyme against  $\beta$ -lactam antibiotics yet resists the inhibitory action of the clinically used inhibitors. These enzymes have come to be known as inhibitor-resistant  $\beta$ -lactamases. The first of these inhibitor-resistant  $\beta$ -lactamases was reported from France in 1992,<sup>5</sup> a mere seven years after introduction of clavulanate to the clinic.

We describe herein properties of one of these inhibitor-resistant  $\beta$ -lactamases, namely the clinically identified M69L mutant variant of the TEM-1  $\beta$ -lactamase from *Escherichia coli*. In a set of observations, we note that the kinetics of turnover of  $\beta$ -lactam substrates, many of the parameters for processing of the inhibitors by the enzyme, and the high-resolution X-ray structure of the mutant enzyme were unaffected compared to those of the wild-type TEM-1  $\beta$ -lactamase. The significant change appears to be a modest reduced affinity of the M69L  $\beta$ -lactamase for the inhibitors, which impairs the formation of the pre-acylation complex. In contrast to the X-ray coordinates, which provide a snapshot of the enzyme, molecular dynamics simulations of the mutant and wild-type enzymes revealed them to be different. Additional computations based on a thermodynamic cycle were used to estimate the free energy of binding of clavulanate to the TEM-1  $\beta$ -lactamase and its M69L variant (also known as TEM-33). It was found that the major contribution to the decrease in affinity as a result of mutation at residue 69 arises due mostly to the electrostatics and van der Waals components of the binding free energy. The effects are small but sufficient for the manifestation of the inhibitor-resistant trait.

## Experimental Procedures

Penicillin G was purchased from Sigma, and clavulanate was obtained from the SmithKline Beecham Pharmaceutical Co. Sulbactam was obtained from Pfizer and tazobactam from Wyeth-Ayerst. All kinetics measurements were performed on a Hewlett-Packard 8453 diodearray spectrophotometer. Calculations of kinetic constants were performed by the MS Excel software. The TEM-1  $\beta$ -lactamase and the M69L mutant variant were purified as described by Vakulenko and Golemi.<sup>6</sup>

**Site-Directed Mutagenesis.** Site-directed mutagenesis of the TEM-1  $\beta$ -lactamase gene was performed with double-stranded DNA of pTZ19-4 using the Transformer Site-Directed Mutagenesis Kit (Clontech). Two primers were used for this purpose: a selection primer (GCATAAGCTATTGCCATTCTC), which mutates the recognition sequence for a unique *Hind*III restriction endonuclease site in the kanamycin resistance gene of the plasmid, and mutagenic primer TEM-69L (CTTTAAAAGTGCTCAGCATTGGAAAACGTTTC), which mutated the AUG codon for methionine at position 69 of the TEM-1  $\beta$ -lactamase to CUG for leucine. Following mutagenesis, DNA was introduced into *E. coli* JM83 by transformation, and mutants were selected on agar containing kanamycin. Six transformants and the strain

producing the wild-type enzyme (control) were checked for resistance to ampicillin in combination with clavulanic acid (fixed concentration of 2  $\mu$ g/mL). The TEM-1  $\beta$ -lactamase gene for two transformants that showed higher levels of resistance than that of the control strain was sequenced.

**Kinetic Determinations.** The assays were carried out by monitoring hydrolysis of penicillin G at 240 nm ( $\Delta\epsilon_{240} = 570 \text{ M}^{-1} \text{ cm}^{-1}$ ). Determination of the inhibition parameters was carried out at room temperature in 100 mM sodium phosphate buffer, pH 7.0. These experiments were performed under conditions of excess substrate concentrations, as described by Koerber and Fink.<sup>7</sup>

Inactivation constants for clavulanate and sulbactam were calculated for both the wild-type and mutant enzymes according to Swaren et al.<sup>8</sup> Inactivation experiments were initiated by the addition of a portion of a stock solution of clavulanate or sulbactam (0.3–3.0 mM final concentration) to the enzyme (2  $\mu$ M) solutions. For tazobactam, the final concentration in the inactivation experiment with wild-type enzyme ranged from 8 to 42  $\mu$ M and with the mutant enzyme from 60 to 300  $\mu$ M. Incubation was terminated by dilution of 10- $\mu$ L aliquots of the mixture into 1 mL of assay solution containing 2 mM penicillin G at various time intervals. The residual enzyme activity in the aliquot was monitored until complete depletion of the substrate resulted. A progressive increase of the activity of the enzyme was observed initially, attributed to its recovery from the transiently inhibited species. The highest steady-state rates in the course of substrate hydrolysis were used in the calculation of the remaining enzyme activity.

The dissociation constants ( $K_i$ ) for all three inhibitors were calculated for the M69L mutant enzyme by the method of Dixon.<sup>9</sup> Two concentrations of the substrate penicillin G, 500 and 800  $\mu$ M, were used. A series of assay mixtures containing both substrate and various concentrations of the inactivators (2–24  $\mu$ M for clavulanate, 2–30  $\mu$ M for sulbactam, and 0.4–2  $\mu$ M for tazobactam) were prepared in 100 mM sodium phosphate buffer, pH 7.0. An aliquot of the stock solution of the enzyme was added to afford a final concentration of 5 nM of the mutant enzyme, in a total volume of 1.0 mL, followed by the immediate measurement of enzyme activity. The rates were measured for the first 5% of substrate turnover.

The partition ratios ( $k_{\text{cat}}/k_{\text{inact}}$ ) for clavulanate, sulbactam, and tazobactam were determined by the titration method.<sup>10</sup> Several buffered mixtures containing various molar ratios [I]/[E] of each of the inhibitors with each of the enzymes were incubated at 4  $^{\circ}\text{C}$  overnight (ca. 20 h). The molar ratio [I]/[E] for clavulanate was varied from 1 to 160. For sulbactam the molar ratio was varied from 1 to 4000, and for tazobactam the molar ratio was varied from 1 to 560. The remaining activity of the enzyme was assayed under conditions of the excess substrate with penicillin G.

The rate constants for recovery of the enzyme activity ( $k_{\text{rec}}$ ) from the transiently inhibited species for the mutant enzyme incubated with each of the compounds were measured at the molar ratio ([I]/[E]) that gave the longest interval of time prior to arrival at a linear steady-state rate for hydrolysis of penicillin G. The calculations of the constants were performed according to the method of Glick et al.<sup>11</sup>

**Steady-State Kinetic Measurements for Substrate Turnover.** The steady-state kinetic parameters for penicillins and cephalosporins were determined from Lineweaver–Burk plots from data for the first 5% of turnover of substrates. The assays were carried out in 100 mM sodium phosphate buffer, pH 7.0, at room temperature. Hydrolyses of substrates were monitored at the following wavelengths: penicillin G at 240 nm ( $\Delta\epsilon_{240} = 570 \text{ M}^{-1} \text{ cm}^{-1}$ ), ampicillin at 235 nm ( $\Delta\epsilon_{235} = 820 \text{ M}^{-1} \text{ cm}^{-1}$ ),

(7) Koerber, S. C.; Fink, A. L. *Anal. Biochem.* **1987**, *165*, 75.

(8) Swarén, P.; Golemi, D.; Cabantous, S.; Bulychev, A.; Maveyraud, L.; Mobashery, S.; Samama, J. P. *Biochemistry* **1999**, *38*, 9570.

(9) Dixon, M. *Biochem. J.* **1953**, *55*, 170.

(10) Silverman, R. *Mechanism-Based Enzyme Inactivation: Chemistry and Enzymology*; CRC Press: Boca Raton, FL, 1988.

(11) Glick, B. R.; Brubacher, L. J.; Leggett, D. J. *Can. J. Biochem.* **1978**, *56*, 1055.

(5) Vedel, G.; Belaouaj, A. C.; Gilly, L.; Philippon, A.; Nevot, P.; Paul, G. *J. Antimicrob. Chemother.* **1992**, *30*, 449.

(6) Vakulenko, S. B.; Golemi, D. *Antimicrob. Agents Chemother.* **2002**, *46*, 646.

**Table 1.** Data Processing and Crystallographic Refinement Statistics

	resolution (Å)	
	37.8–1.59	1.65–1.59
observations	251 413	5 055
unique reflections	30 309	2 145
multiplicity	8.3	2.4
completeness	96.4	70.3
% of reflections with $I/\sigma < 3$	4.1	10.5
$R_{\text{sym}}$	0.070	0.065
$R$ factor		0.133
$R_{\text{free}}$		0.175
rmsd bond length (Å)		0.01
rmsd angle (°)		1.45

piperacillin at 230 nm ( $\Delta\epsilon_{230} = 1000 \text{ M}^{-1} \text{ cm}^{-1}$ ), cephaloridine at 267 nm ( $\Delta\epsilon_{267} = 1000 \text{ M}^{-1} \text{ cm}^{-1}$ ), cephalothin at 270 nm ( $\Delta\epsilon_{270} = 3250 \text{ M}^{-1} \text{ cm}^{-1}$ ), and cephalosporin C at 280 nm ( $\Delta\epsilon_{280} = 2390 \text{ M}^{-1} \text{ cm}^{-1}$ ). In all cases, substrate concentrations flanked the  $K_m$  values.

**Crystallization.** The M69L mutant TEM  $\beta$ -lactamase was crystallized according to the procedure described for the wild-type TEM-1 enzyme.<sup>12</sup> Briefly, 1  $\mu\text{L}$  of 33% saturated ammonium sulfate and 0.01% sodium azide in 25 mM sodium potassium phosphate buffer (pH 7.8) was added to a 3- $\mu\text{L}$  droplet of protein solution at 25 mg/mL in the same buffer. The droplet was equilibrated against a 500- $\mu\text{L}$  reservoir solution made of 41% saturated ammonium sulfate, 4% (v/v) acetone buffered with 100 mM sodium potassium phosphate at pH 7.8. After equilibration, the clear drop was seeded with a wild-type crystal (about  $100 \times 50 \times 50 \mu\text{m}^3$ ), and the ammonium sulfate concentration of the reservoir was gradually increased to 49% in 1% increments. At the end of this procedure, the crystal reached a size of  $400 \times 400 \times 500 \mu\text{m}^3$ . Acetone was slowly evaporated, and the crystal was cryoprotected by a short immersion in a 50% (w/v) PEG 20 000 solution before being cooled in a nitrogen gaseous flux at 100 K.

**Data Collection and Processing.** Diffraction data to 1.6 Å resolution were collected using a Mar CCD scanner on beamline BM30A at ESRF (Grenoble, France) and at a wavelength of 0.9796 Å. Two data sets ( $180^\circ$  rotation for each of them) were measured for the high- and the low-resolution data, respectively. The frames were indexed, integrated, and scaled with the HKL package.<sup>13</sup> Intensities were converted to amplitudes using TRUNCATE from the CCP4 suite of programs.<sup>14</sup> Relevant statistics are presented in Table 1. Crystals of the mutant variant were isomorphous to those of the TEM-1  $\beta$ -lactamase,<sup>15</sup> with cell parameters  $a = 41.78 \text{ \AA}$ ,  $b = 62.18 \text{ \AA}$ , and  $c = 88.52 \text{ \AA}$  in the orthorhombic  $P2_12_12_1$  space group.

**Structure Refinement.** Five percent of the data were randomly selected and excluded from refinement as a test set for the  $R_{\text{free}}$  calculation. An initial step of rigid body refinement was performed at 3.0 Å resolution using the refined TEM-1  $\beta$ -lactamase structure as a starting model, after removal of all side-chain atoms at position 69. Further refinement of the structure of the M69L enzyme was performed using the maximum likelihood method as implemented in REFMAC.<sup>16</sup> Model building and manual corrections were carried out using TURBO-FRODO and included anisotropic  $B$  factor refinement. The SigmaA-weighted electron density maps computed after the first step of refinement clearly indicated the presence of a leucine residue at position 69. Water molecules were automatically added to the model using ARP.

The final structure of the M69L mutant TEM-1  $\beta$ -lactamase was comprised of 2035 non-hydrogen atoms, 535 water molecules built as

neutral oxygen atoms, and 2 sulfate anions. The values of the  $R$  and  $R_{\text{free}}$  factors were 0.132 and 0.175, respectively, for all reflections between 37.8 and 1.60 Å resolution.

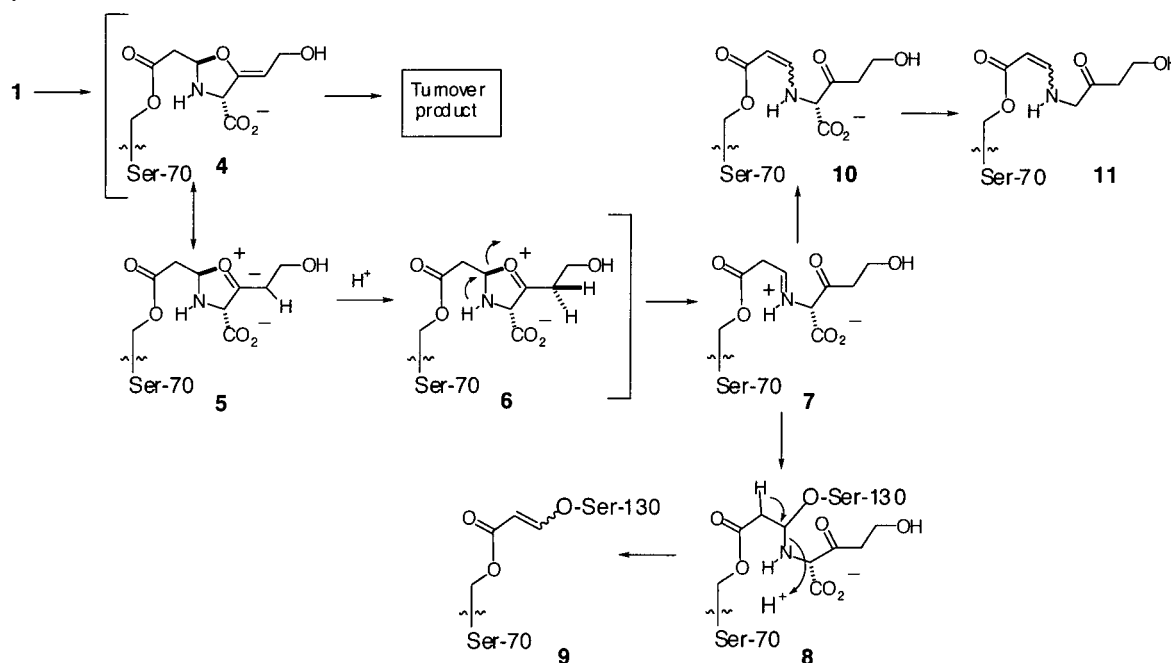
**Molecular Dynamics and Correlation Analyses.** A model of the pre-acylation complex of the wild-type TEM-1 and clavulanate was previously constructed<sup>17</sup> on the basis of the X-ray structures of the native TEM-1  $\beta$ -lactamase (PDB accession code 1BTL). A model of the M69L/clavulanate pre-acylation complex was also developed. This process was carried out with the aid of the SYBYL 6.7 package (Tripos Inc., 1699 S. Hanley Rd., St. Louis, MO 63144). The two complexes, one with the wild-type and the other with the mutant enzyme, were then immersed in a TIP3P water box, at least 10 Å from any face of the box. Preparation of the complexes for molecular dynamics simulations was based on a protocol described previously.<sup>18</sup> The particle mesh Ewald (PME) method was used to treat long-range electrostatics.<sup>19</sup> Bonds that involved hydrogen atoms were constrained with SHAKE, and a time step of 2 fs was used to carry out molecular dynamics simulations.<sup>20</sup> The total number of atoms in the solvated TEM-1/clavulanate system was 37 030, two atoms less than in the solvated M69L/clavulanate system. All energy minimizations and molecular dynamics simulations of the enzyme/clavulanate complexes were carried out using the Sander module within the AMBER 6 suite of programs.<sup>21</sup> Force-field parameters and atomic charges for standard protein residues were taken from Cornell et al.<sup>22</sup> Atomic charges for clavulanate were determined using the RESP fitting procedure.<sup>23</sup> A HF/6-31G\* single-point energy calculation was done to determine the electrostatic potential around the molecule, which was subsequently used in the two-stage RESP fitting procedure. All ab initio calculations were carried out using the Gaussian 98 suite of programs.<sup>24</sup> Following equilibration, two separate 2-ns molecular dynamics simulations at constant pressure and temperature (300 K) were carried out for the M69L mutant/clavulanate and wild-type TEM-1/clavulanate complexes. Snapshots were collected for analysis every 0.2 ps. Dynamic cross-correlation maps (DCCM) were generated from the trajectories on the basis of the procedure described by Ichiye and Karplus.<sup>25</sup> Elements of the cross-correlation matrix were computed using a combination of software packages, including the ptraj module within the AMBER package, SYBYL 6.7, and an in-house program.

**Binding Free Energy Calculations.** The method for determination of the free energy of binding has been described.<sup>26–29</sup> The method is a combination of molecular mechanics, Poisson–Boltzmann electrostat-

- (12) Jelsch, C.; Lenfant, F.; Masson, J. M.; Samama, J. P. *J. Mol. Biol.* **1992**, *223*, 377.  
 (13) Otwinowski, Z.; Minor, W. Processing of X-ray diffraction data collected in oscillation mode. *Methods Enzymol.* **1997**, *276*, 307.  
 (14) Bailey, S. *Acta Crystallogr.* **1994**, *D50*, 760.  
 (15) Jelsch, C.; Mourey, L.; Masson, J. M.; Samama, J. P. *Proteins* **1993**, *16*, 364.  
 (16) Murshudov, G. N.; Vagin, A. A.; Dodson, E. J. *Acta Crystallogr.* **1997**, *D53*, 240.

- (17) Vakulenko, S. B.; Geryk, B.; Kotra, P. L.; Mobashery, S.; Lerner, S. A. *Antimicrob. Agents Chemother.* **1998**, *42*, 1542.  
 (18) Maveyraud, L.; Golemi, D.; Ishiwata, A.; Meroueh, O.; Mobashery, S.; Samama, J.-P. *J. Am. Chem. Soc.* **2002**, *124*, 2461.  
 (19) Darden, T. A.; York, D. M.; Pedersen, L. G. *J. Chem. Phys.* **1993**, *98*, 10089.  
 (20) Ryckaer, J. P.; Ciccotti, G.; Berendsen, J. H. C. *J. Comput. Chem.* **1977**, *23*, 327.  
 (21) Case, D. A.; Pearlman, D. A.; Caldwell, J. W.; Cheatham, T. E., III; Ross, W. S.; Simmerling, C. L.; Darden, T. A.; Merz, K. M.; Seibel, G. L.; Cheng, A. L.; Vincent, J. J.; Crowley, M.; Tsui, V.; Radmer, R. J.; Duan, Y.; Pitera, J.; Massova, I.; Seibel, G. L.; Singh, U. C.; Weiner, P. K.; Kollman, P. A. (1999) AMBER 6, University of California, San Francisco.  
 (22) Cornell, W. D.; Cieplak, P.; Bayley, C. I.; Gould, I. R.; Merz, K. M.; Ferguson, D. M.; Spellmeyer, D. C.; Fox, T.; Caldwell, J. W.; Kollman, P. A. *J. Am. Chem. Soc.* **1995**, *117*, 5179.  
 (23) Bayly, C. I.; Cieplak, P.; Cornell, W. D.; Kollman, P. A. *J. Chem. Phys.* **1993**, *97*, 10269.  
 (24) Frisch, M. J.; Trucks, G. W.; Schlegel, H. B.; Scuseria, G. E.; Robb, M. A.; Cheeseman, J. R.; Zakrzewski, V. G.; Montgomery, J. A., Jr.; Stratmann, R. E.; Burant, J. C.; Dapprich, S.; Millam, J. M.; Daniels, A. D.; Kudin, K. N.; Strain, M. C.; Farkas, O.; Tomasi, J.; Barone, V.; Cossi, M.; Cammi, R.; Mennucci, B.; Pomelli, C.; Adamo, C.; Clifford, S.; Ochterski, J.; Petersson, G. A.; Ayala, P. Y.; Cui, Q.; Morokuma, K.; Malick, D. K.; Rabuck, A. D.; Raghavachari, K.; Foresman, J. B.; Cioslowski, J.; Ortiz, J. V.; Stefanov, B. B.; Liu, G.; Liashenko, A.; Piskorz, P.; Komaromi, I.; Gomperts, R.; Martin, R. L.; Fox, D. J.; Keith, T.; Al-Laham, M. A.; Peng, C. Y.; Nanayakkara, A.; Gonzalez, C.; Challacombe, M.; Gill, P. M. W.; Johnson, B. G.; Chen, W.; Wong, M. W.; Andres, J. L.; Head-Gordon, M.; Replogle, E. S.; Pople, J. A. *Gaussian 98*, Gaussian, Inc.: Pittsburgh, PA, 1998.  
 (25) Ichiye, T.; Karplus, M. *Proteins* **1991**, *11*, 205.  
 (26) Wang, W.; Wendell, A. L.; Araz, J.; Jian, W.; Wang, J.; Luo, R.; Bayly, C. I.; Kollman, P. A. *J. Am. Chem. Soc.* **2001**, *123*, 3986.

Scheme 1

**Table 2.** Kinetics Parameters for the Interactions of the Wild-Type TEM-1  $\beta$ -Lactamase and Its M69L Variant with the Clinically Used Inhibitors

enzyme	inhibitor	$k_{\text{cat}}$ ( $\text{s}^{-1}$ )	$k_{\text{inact}}$ ( $\text{s}^{-1}$ ) $\times 10^2$	$K_i$ ( $\mu\text{M}$ )	$k_{\text{cat}}/k_{\text{inact}}$	$k_{\text{rec}}$ ( $\text{s}^{-1}$ ) $\times 10^2$
wild-type <sup>a</sup>	clavulanate	$0.21 \pm 0.03$	$0.17 \pm 0.03$	$0.4 \pm 0.1$	$125 \pm 36$	$0.84 \pm 0.01$
	sulbactam	$2.0 \pm 0.2$	$0.020 \pm 0.005$	$1.6 \pm 0.4$	$10000 \pm 3000$	$1.12 \pm 0.02$
	tazobactam	$1.4 \pm 0.9$	$0.3 \pm 0.2$	$0.02 \pm 0.01$	$475 \pm 42$	$0.72 \pm 0.01$
M69L	clavulanate	$15 \pm 4$	$5 \pm 1$	$10 \pm 1$	$300 \pm 51$	$0.14 \pm 0.01$
	sulbactam	$56 \pm 9$	$1.3 \pm 0.2$	$50 \pm 13$	$4320 \pm 193$	$0.23 \pm 0.02$
	tazobactam	$6 \pm 2$	$1.9 \pm 0.1$	$2.6 \pm 0.8$	$330 \pm 101$	$0.4 \pm 0.1$

<sup>a</sup> The data are cited from Swarén et al. (*Biochemistry* **1999**, *38*, 9570–9576).

ics, and surface-accessible calculations (MM-PBSA).<sup>30</sup> As described previously,<sup>30</sup> the binding free energy is expressed as

$$\Delta G_{\text{bind}} = \Delta G_{\text{solv}}^{\text{E}} + \Delta G_{\text{solv}}^{\text{L}} - \Delta G_{\text{solv}}^{\text{EL}} - \Delta G_{\text{MM}} \quad (1)$$

where  $\Delta G_{\text{bind}}$  is the binding free energy,  $\Delta G_{\text{MM}}$  is the free energy of association of the enzyme and ligand in the gas phase, and  $\Delta G_{\text{solv}}^{\text{E}}$ ,  $\Delta G_{\text{solv}}^{\text{L}}$ , and  $\Delta G_{\text{solv}}^{\text{EL}}$  correspond to the solvation free energies of the enzyme (E), clavulanate (L), and enzyme–clavulanate complex (EL), respectively.  $\Delta G_{\text{MM}}$  is given by

$$\Delta G_{\text{MM}} = \Delta E_{\text{MM}} - T\Delta S \quad (2)$$

where  $\Delta E_{\text{MM}}$  is the difference in the sum of bond, angle, dihedral, electrostatic, and van der Waals energies between products and reactants computed with the AMBER force field. The solvation free energy is composed of two terms, namely electrostatics and nonpolar, and is given by

$$\Delta G_{\text{solv}} = \Delta G_{\text{PB}} + \Delta G_{\text{nonpolar}} \quad (3)$$

The electrostatic contribution to the free energy,  $\Delta G_{\text{PB}}$ , is determined using the Delphi software package<sup>31</sup> that numerically solves the Poisson–Boltzmann equations to determine the electrostatic contribution to the solvation free energy. A 0.5-Å grid size was used, and the dielectric constant for the protein and for water were set to 2 and 80, respectively. Atomic radii were taken from the PARSE parameter set, and partial charges were taken from Cornell et al.<sup>22</sup> for standard residues; RESP charges were assigned to nonstandard residues (vide infra). The nonpolar contribution to the solvation free energy was

calculated using the MSMS program<sup>32</sup> according to the method of Sitkoff et al.<sup>33</sup>

The entropy was estimated from normal-mode calculations<sup>27</sup> using the NMODE program within the AMBER suite. Because these calculations are computationally intensive, only residues within 12 Å of clavulanate were considered for the normal-mode analysis of the equilibrated structure.

## Results and Discussion

The process of inhibition of the class A  $\beta$ -lactamases by the clinically used inhibitors is complicated, involving multiple events taking place concurrently. These events are depicted for clavulanate in Scheme 1, but the process is similar for sulbactam<sup>34</sup> and tazobactam.<sup>35</sup> These events have been evaluated (Table 2) in our studies, as will be detailed below.

Clavulanate acylates the active site Ser-70, as would any  $\beta$ -lactamase substrate. At this stage, the acyl–enzyme species may undergo deacylation, as in typical turnover events (4 →

- (27) Wang, J.; Morin, P.; Wang, W.; Kollman, P. A. *J. Am. Chem. Soc.* **2001**, *123*, 5221.
- (28) Wang, W.; Kollman, P. A. *J. Mol. Biol.* **2000**, *303*, 567.
- (29) Srinivasan, J.; Cheatham, T. E., III; Kollman, P. A.; Case, D. A. *J. Am. Chem. Soc.* **1998**, *120*, 9401.
- (30) Massova, I.; Kollman, P. A. *Perspect. Drug Discov.* **2000**, *18*, 113.
- (31) Nicholls, A.; Honig, B. *J. Comput. Chem.* **1991**, *12*, 435.
- (32) Sanner, M. F.; Olson, A. J.; Spehner, J. *Biopolymers* **1996**, *38*, 305.
- (33) Sitkoff, D.; Sharp, K. A.; Honig, B. *J. Phys. Chem.* **1994**, *98*, 1978.
- (34) Imtiaz, U.; Billings, E. M.; Knox, J. R.; Mobashery, S. *Biochemistry* **1994**, *33*, 5728.
- (35) Kuzin, A. P.; Nukaga, M.; Nukaga, Y.; Hujer, A.; Bonomo, R. A.; Knox, J. R. *Biochemistry* **2001**, *40*, 1861.

**Table 3.** Kinetics Parameters for Turnover of Substrates by the Wild-Type TEM-1  $\beta$ -Lactamase and Its M69L Variant

	wild-type TEM-1			M69L TEM-1 variant		
	$k_{\text{cat}}$ ( $\text{s}^{-1}$ )	$K_{\text{m}}$ ( $\mu\text{M}$ )	$K_{\text{cat}}/K_{\text{m}}$ ( $\text{M}^{-1} \text{s}^{-1}$ )	$k_{\text{cat}}$ ( $\text{s}^{-1}$ )	$K_{\text{m}}$ ( $\mu\text{M}$ )	$k_{\text{cat}}/K_{\text{m}}$ ( $\text{M}^{-1} \text{s}^{-1}$ )
benzylpenicillin	$1100 \pm 63$	$24 \pm 1$	$(4.6 \pm 0.3) \pm 10^7$	$2900 \pm 250$	$144 \pm 12$	$(2.0 \pm 0.2) \pm 10^7$
ampicillin	$730 \pm 24$	$31 \pm 1$	$(2.4 \pm 0.1) \pm 10^7$	$2200 \pm 290$	$134 \pm 20$	$(1.6 \pm 0.3) \pm 10^7$
piperecillin	$690 \pm 130$	$33 \pm 6$	$(2.1 \pm 0.5) \pm 10^7$	$1200 \pm 160$	$100 \pm 14$	$(1.2 \pm 0.2) \pm 10^7$
cephaloridine	$1100 \pm 103$	$674 \pm 65$	$(1.6 \pm 0.2) \pm 10^6$	$800 \pm 130$	$1200 \pm 200$	$(7 \pm 2) \pm 10^5$
cephalothin	$130 \pm 10$	$274 \pm 20$	$(4.7 \pm 0.5) \pm 10^5$	$220 \pm 15$	$380 \pm 26$	$(5.7 \pm 0.5) \pm 10^5$

turnover product), or it may undergo a requisite rearrangement for the inactivation event that leads to species **7**. The ring-opening event for clavulanate was shown to require protonation of species **5** (a resonance structure for the intermediate **4**), the source of proton for which is a crystallographically conserved water molecule tethered by the side chain of Arg-244 and the main-chain carbonyl of Val-216.<sup>36,37</sup> Species **7** partitions among species **9**, **10**, and **11**, with roughly similar rate constants in the case of the TEM-1  $\beta$ -lactamase. The tautomerization of **7**  $\rightarrow$  **10** gives rise to the transiently inhibited species, which in turn may result in **11**.<sup>38</sup> Trapping of the side chain of Ser-130 by **7** gives rise to species **8**, which leads to the transformation **8**  $\rightarrow$  **9**.<sup>39,40</sup> Species **9** accounts for the irreversibly inhibited enzyme, which links two active-site serine residues to the several atoms from the inhibitor molecule. The chemistry of enzyme inhibition is the same for sulbactam and tazobactam, except the five-membered ring-opening event in those cases takes place unassisted by the enzyme.<sup>34,41</sup> Hence, it is plausible that a mechanism that leads to resistance to inhibition by disrupting a given step of this process (Scheme 1) for one inhibitor should likely result in the same for the other two inhibitors.

**Enzyme Inactivation and Turnover of Inhibitors.** It is interesting to note that the M69L mutant TEM-1 turned over all three inhibitors (Table 2) better than did the wild-type enzyme (e.g.,  $k_{\text{cat}}$ ). This was especially true for clavulanate, which was turned over better by the mutant enzyme by 71-fold. Interestingly, the rate constant for enzyme inactivation ( $k_{\text{inact}}$ ) was also enhanced for all three inhibitors. The net effect was that the partition ratios (i.e.,  $k_{\text{cat}}/k_{\text{inact}}$ ), a measure of the efficiency of the enzyme inactivation process, did not change significantly for any of the three enzyme inhibitors. The transiently inhibited species (**10**) has been well documented in inhibition of  $\beta$ -lactamases by these inhibitors. When this species undergoes hydrolysis at the ester group, recovery of enzyme activity takes place. The rate constants for recovery of activity from this species ( $k_{\text{rec}}$ ) generally were not appreciably different for all three inhibitors with the wild-type enzyme. Similarly, comparison of the  $k_{\text{rec}}$  values for the wild-type and mutant enzymes did not show any substantial difference. These observations argue for the similarity of the process for recovery of activity from the transiently inhibited species among the three species for the various inhibitors.

It would appear that the parameter that accounts for the inhibitor-resistant trait for the M69L mutant variant is the simple affinity of the enzyme active site for the inhibitors. That is to

say, the formation of the noncovalent pre-acylation complex between the inhibitor and the enzyme is impaired. The dissociation constant ( $K_1$ ) for the three inhibitors measured for the mutant enzyme invariably increased compared to the wild-type values. The increase ranged from 24- to 130-fold, with the highest increase measured for tazobactam. However, since the wild-type enzyme showed the highest affinity for tazobactam ( $K_1 = 20$  nM), the increase by 130-fold in the dissociation constant brought the value to the lower micromolar range.

**Catalytic Ability of the Inhibitor-Resistant  $\beta$ -Lactamase in Turnover of Typical Antibiotic Substrates.** Table 3 summarizes the results of steady-state turnover for three penicillins and two cephalosporins. The incremental differences are small and essentially negligible. It is interesting that both  $k_{\text{cat}}$  and  $K_{\text{m}}$  values in general increased for the mutant enzyme. The largest effect on  $k_{\text{cat}}$  was seen for ampicillin (3-fold) and on  $K_{\text{m}}$  for benzylpenicillin (6-fold). The consequent effects on the ratios for  $k_{\text{cat}}/K_{\text{m}}$  are vanishingly small. The two enzymes are essentially equally competent in turnover of  $\beta$ -lactam substrates; hence, the mutation did not alter the normal function of the TEM-1  $\beta$ -lactamase in the least.

**High-Resolution X-ray Structure.** The overall three-dimensional structure of the M69L variant of the TEM-1  $\beta$ -lactamase is essentially identical to that of the wild-type enzyme. The rms deviations for the 1052 main-chain atoms was 0.57 Å, and it was 0.72 Å when all protein atoms were considered.

A detailed comparison in the vicinity of the mutation site indicated that the M69L mutation induces a very small displacement of the main-chain atoms of R244 and of the neighboring residues on  $\beta$ -strand S4 (Figure 1), but the position of the side-chain atoms did not change compared to the wild-type enzyme. Another feature in the structure of the M69L variant is the absence of the sulfate anion bound in the active site (Figure 2), in the location corresponding to the inhibitor carboxylate. As will be discussed, this factor is likely to be the result of the altered electrostatic features of the enzyme surface within the active site. A similar observation was made in the structure of the N276D mutant of the TEM-1 enzyme, another inhibitor-resistant TEM  $\beta$ -lactamase.<sup>8</sup>

**Molecular Dynamics Simulations.** Substitution of methionine by leucine is remarkable in its seeming benignness (Figures 1 and 2).<sup>42</sup> The essence of the structure alteration is a shortening of the side chain at position 69 by a fraction of an angstrom. This is a conservative change in the protein that not only did not alter the X-ray structure of the enzyme but indeed preserved the full catalytic competency of the  $\beta$ -lactamase. The M69L  $\beta$ -lactamase is as fully active as the wild-type enzyme (Table 3).

(36) Imtiaz, U.; Billings, E.; Knox, J. R.; Manavathu, E. K.; Lerner, S. A.; Mobashery, S. *J. Am. Chem. Soc.* **1993**, *115*, 4435.

(37) Miyashita, K.; Massova, I.; Mobashery, S. *Bioorg. Med. Chem. Lett.* **1995**, *6*, 319.

(38) Chen, C. C.; Herzberg, O. *J. Mol. Biol.* **1992**, *224*, 1103.

(39) Brown, R. P.; Alpin, R. T.; Schofield, C. J. *Biochemistry* **1996**, *35*, 12421.

(40) Brown, R. P.; Alpin, R. T.; Schofield, C. J. *J. Antibiot.* **1997**, *50*, 184.

(41) Yang, Y.; Janota, K.; Tabei, K.; Huang, N.; Marshall, M. S.; Lin, Y.-I.; Rasmussen, B. A.; Shlaes, D. M. *J. Biol. Chem.* **2000**, *275*, 26674.

(42) Chaibi, E. B.; Péduzzi, J.; Farzaneh, S.; Barthélémy, M.; Sirot, D.; Labia, R. *Biochim. Biophys. Acta* **1998**, *1382*, 38.

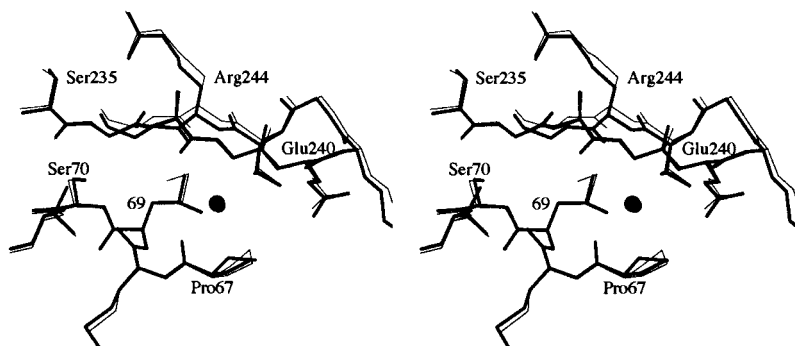


**Figure 1.** Superimposition of the structure of the TEM-1  $\beta$ -lactamase (thin lines) and of the M69L TEM mutant (thick lines) in the vicinity of the mutation site. A water molecule, conserved in both structures, is represented as a black sphere.

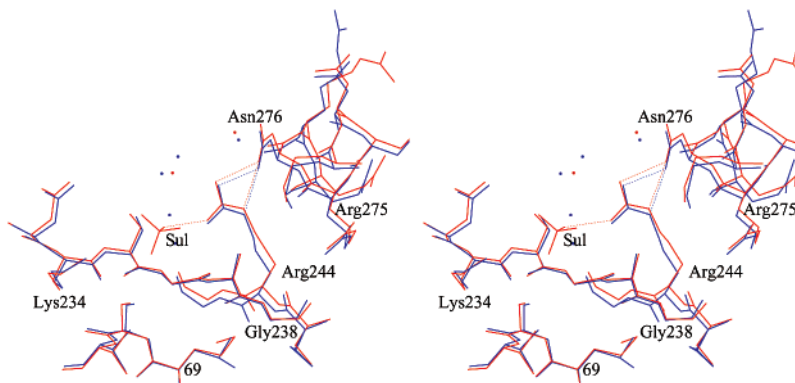


**Figure 2.** Superimposed stereoview of the structure of the active site of the TEM-1  $\beta$ -lactamase (red) and of the M69L mutant variant (blue). The sulfate anion ("Sul"), present only in the active site of the wild-type enzyme, is labeled. Water molecules are depicted as dots of corresponding colors. Hydrogen bonds involving the side chain of R244 in each case are represented as dotted lines.

In the absence of any obvious factor that could account for the inhibitor-resistant property of the M69L variant from the high-resolution X-ray structure, we felt that the difference between the two enzymes must rest in their dynamic behaviors. Given that residue 69 is not directly involved in interactions with the inhibitors, it appeared plausible to us that the mutation might be affecting inhibitor binding properties of the enzyme either through adjacent residue-to-residue fluctuations or by altering global motions of the protein.

A dynamic cross-correlated map was computed from individual 2-ns molecular dynamics simulations of the TEM-1  $\beta$ -lactamase and its M69L variant, as depicted in Figure 3. These maps provide detailed information about the correlation between the fluctuations of the positions of the residues and secondary structural elements in the two proteins. Cross-correlation coefficients ranged from  $-1$  to  $+1$ . Negative values correspond to anticorrelated motions, where residues are generally moving in opposite directions. In contrast, positive values correspond to correlated motions, during which residues are generally moving in the same direction.

For the ensuing discussion, we use the terminology for the helices and  $\beta$ -strands according to Jelsch et al.,<sup>15</sup> as depicted in Figure 3A. Adjacent elements in the protein structure are expected to result in positive correlations.<sup>25</sup> As presented in Figure 3B,C, H2 helix (amino acids 69–85), which contains residue M69 and the catalytically important S70, moved in phase (correlated motion) with the spatially adjacent helices H4 (spanning residues 119–128) and H9 (spanning residues 201–212), and  $\beta$ -sheet S3 (spanning residues 230–237). Anticorrelated motions were found in several locations throughout (Figure 3B,C), but regions of strong anticorrelated motion remained very

limited (e.g., residues 86–88 and residues 189–192). Data presented in Figure 3B,C revealed an overall seemingly similar patterns of correlated and anticorrelated motions.

In the absence of any strong overall discernible differences in the collective motions of the two proteins, we resorted to analyses of the motion of residue 69 with respect to the motions of the other amino acids by taking a cross section of Figure 3B,C at position 69. In essence, whether the motion of residue 69 with reference to other residues is in the same direction (i.e., correlated motion) or is in the opposing direction (i.e., anticorrelated) is documented in Figure 4A,B. Motions of spatially adjacent residues are expected to be correlated. The motion among residues adjacent to L69 (in the mutant variant) were more strongly correlated than those of M69 (in the wild-type). It is of interest to note the disappearance of anticorrelated motion with respect to residue 69 from the  $\Omega$  loop of the mutant enzyme (white arrows Figure 4A,B). This loop (spanning residues 162–179) is believed to play an important role in substrate turnover<sup>1</sup> because of E166, the general base that promotes deacylation of the intermediacy acyl–enzyme species in the course of substrate turnover.<sup>1,43–47</sup> Furthermore, anticorrelated motions with respect to residue 69 in the mutant enzyme disappeared almost entirely in the H6 helix (yellow arrows in Figure 4A,B) and in a loop (L2) connecting H6 with the  $\Omega$  loop. Additional anticorrelated

(43) Lietz, E. J.; Truher, H.; Kahn, D.; Hokenson, J. M.; Fink, A. L. *Biochemistry* **2000**, *39*, 4971.

(44) Mourey, L.; Miyashita, K.; Swarén, P.; Bulychev, A.; Samama, J. P.; Mobashery, S. *J. Am. Chem. Soc.* **1998**, *120*, 9383.

(45) Strynadka, N. C. J.; Adachi, H.; Jensen, S. E.; Johns, K.; Sielecki, A.; Betzel, C.; Sutoh, K.; James, M. N. G. *Nature* **1992**, *359*, 700.

(46) Maveyraud, L.; Massova, I.; Birck, C.; Miyashita, K.; Samama, J. P.; Mobashery, S. *J. Am. Chem. Soc.* **1996**, *118*, 7435.

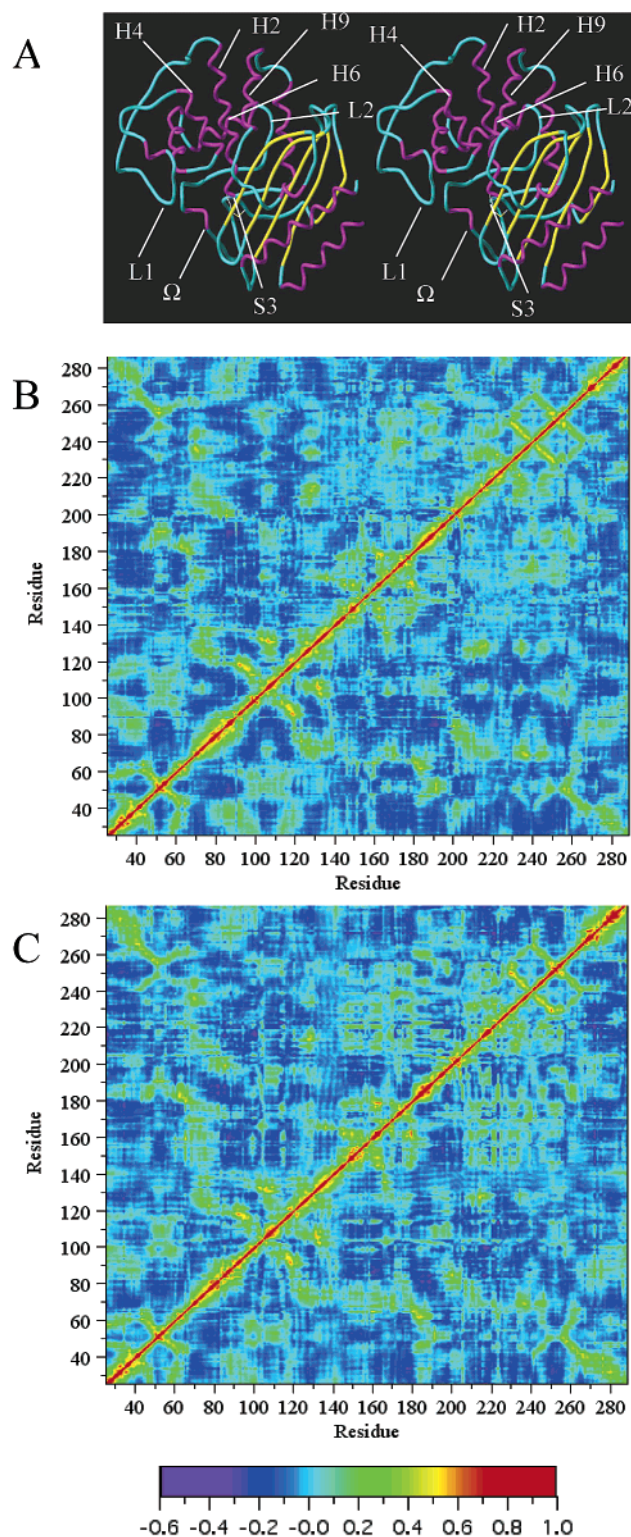


**Figure 3.** (A) Tube rendering of the TEM-1  $\beta$ -lactamase color-coded according to secondary structure: purple for helices, yellow for strands, and the rest in cyan. The residue-to-residue dynamic cross-correlated maps for (B) the wild-type TEM-1  $\beta$ -lactamase and (C) the M69L variant. The color-coded bar indicates the spectrum of dynamics motions for the correlated (from red) to anticorrelated (to magenta).

motion appeared in a portion of a large loop (L1) that borders the active site (orange arrow in Figure 4A,B).

(47) Guillaume, G.; Vanhove, M.; Lamotte-Brasseur, J.; Ledent, P.; Jamin, M.; Joris, B.; Frère, J. M. *J. Biol. Chem.* **1997**, *272*, 5438.

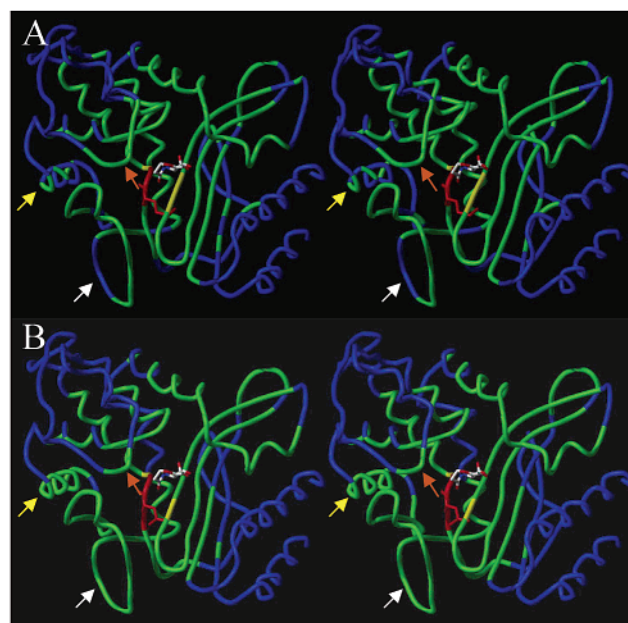


**Figure 4.** Tube rendering of the backbone of the (A) TEM-1  $\beta$ -lactamase and (B) the M69L variant, where amino acid positions are color-coded according to cross-correlation coefficients from a cross section of the dynamic cross-correlated map at residue 69. Coloring is based on the color bar given in Figure 3. A model of clavulanate bound to the active site in the preacylation complex is given in both images.

Figure 5 documents the rms deviations of the L2 and  $\Omega$  loops (combined), the L1 loop, and the H6 helix as a function of time. It would appear that the motions of these regions are different for the wild-type and mutant enzymes. In the case of the L2 and  $\Omega$  loop, Figure 5A shows large fluctuations of the rms deviations in the TEM-1 structure for the first nanosecond of simulation. It would appear that the  $\Omega$  loop underwent a major conformational change at  $\sim 500$  ps and the resulting structure remained stable for an additional 500 ps. Concurrent with this event, the distance between the center-of-mass of the  $\Omega$  loop to residue 69 in the wild-type enzyme increased by  $0.7 \text{ \AA}$ , a change in the structure not seen for M69L mutant. The rms deviations were more pronounced in the loop spanning residues 96–108 (Figure 5B), where the mean rms deviations consistently remained greater in the wild-type in the last 1.5 ns of the simulations. The rms deviations of the H6 helix (Figure 5C) also showed larger deviations of the values of TEM-1 beyond the first 500 ps of simulation.

Therefore, despite the many similarities of the X-ray structures for the wild-type and mutant  $\beta$ -lactamases, the dynamic motions of the two proteins show differences in the vicinity of the active sites (e.g., the  $\Omega$  and L1 loops), underscoring the concept that biological catalysts rely on dynamic motion in the course of catalysis. In the case of the TEM-1  $\beta$ -lactamase, the dynamic motions of residues in the vicinity of the active site were found to be related to those of residues at locations remote from the active site (H6 helix and L2 loop).

**Binding Free Energy.** Free energy perturbation methods<sup>48,49</sup> have been extensively used to evaluate binding free energies, in some cases within  $\sim 1$  kcal/mol of the experimental results.<sup>50</sup>

(48) Kollman, P. A. *Chem. Rev.* **1993**, *93*, 2395.

(49) Beveridge, D. L.; DiCapua, F. M. *Annu. Rev. Biophys. Biomol. Struct.* **1983**, *18*, 431.

(50) Rao, B. G.; Kim, E. E.; Murcko, M. A. *J. Comput.-Aided Mol. Des.* **1996**, *10*, 23.

**Table 4.** Free Energy of Binding for the Formation of the Pre-acylation Complexes of Clavulanate and the TEM-1  $\beta$ -Lactamase and of Clavulanate and the M69L Mutant Variant (All Energies in kcal/mol)<sup>a</sup>

	$\Delta E^{\text{vdw}}$	$\Delta E^{\text{elec}}$	$T\Delta S$	$\Delta G^{\text{PB}}$	$\Delta G^{\text{SA}}$	$\Delta G^{\text{calc}}$	$\Delta\Delta G_{\text{bind}}^{\text{calc}}$	$\Delta\Delta G_{\text{bind}}^{\text{exp}}$
wild-type	$-21.1 \pm 0.2$	$-90.2 \pm 0.9$	13.0	$77.6 \pm 0.7$	$-3.3 \pm 0.1$	$-24.0 \pm 0.4$		
M69L	$-19.4 \pm 0.2$	$-94.0 \pm 0.8$	10.1	$84.1 \pm 0.5$	$-3.3 \pm 0.1$	$-22.6 \pm 0.4$	$1.4 \pm 0.6$	$1.9 \pm 0.2$

<sup>a</sup>  $\Delta E^{\text{vdw}}$ , van der Waals potential energy;  $\Delta E^{\text{elec}}$ , electrostatic potential energy;  $\Delta S$ , the entropy;  $\Delta G^{\text{PB}}$ , electrostatic contributions to the solvation free energy;  $\Delta G^{\text{SA}}$ , nonpolar contributions to solvation free energy.  $\Delta\Delta G_{\text{bind}}^{\text{calc}}$ , change in the calculated free energy of binding;  $\Delta\Delta G_{\text{bind}}^{\text{exp}}$ , change in the experimentally determined free energy of binding.

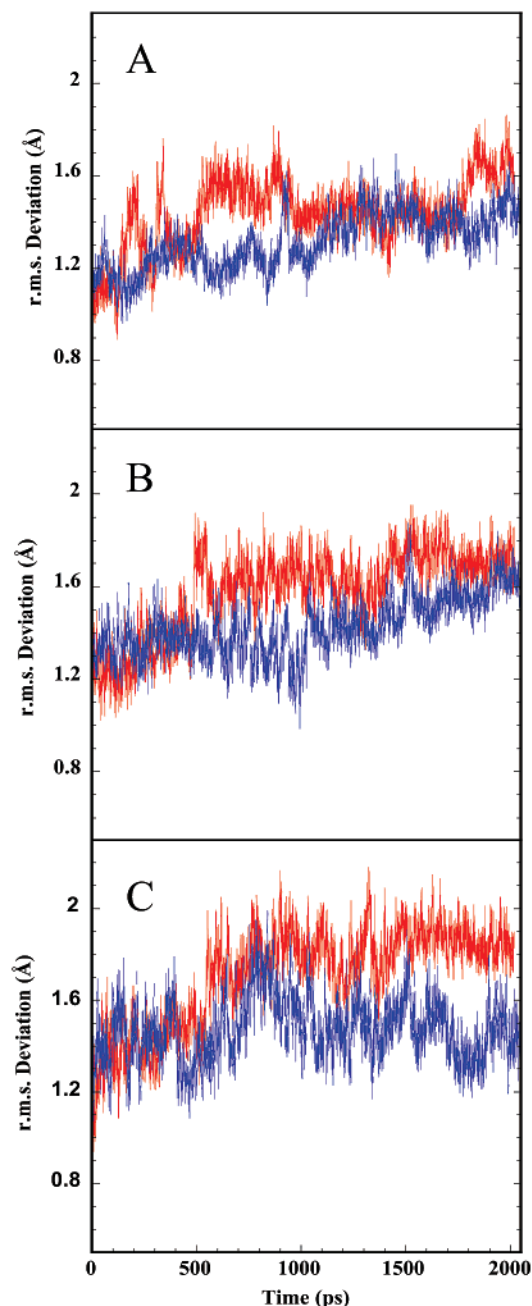


**Figure 5.** Root-mean-square deviations (Å) of (A) the loop spanning residues 155–161 (L2) and  $\Omega$  loop, of (B) the loop spanning residues 96–108 (L1), and of (C) the H6  $\alpha$ -helix of the wild-type TEM-1 and its M69L variant for the course of the 2 ns molecular dynamics simulations (red corresponds to wild-type and blue to M69L mutant).

At the other end of the spectrum, numerous empirical functions<sup>51–53</sup> have been developed to rapidly rank in some cases

hundreds of thousands of compounds in virtual screening experiments. Recently, Srinivasan et al.<sup>29</sup> have introduced a semiempirical method, which was subsequently termed MM-PBSA,<sup>30</sup> for computing binding free energies. The method has been used extensively to study protein–ligand and protein–protein interactions.<sup>29,30,54</sup> This method can be used with compounds that are very different from one another.<sup>28</sup> The binding free energy is computed by combining polar and nonpolar contributions to the solvation free energy, energies from electrostatic and van der Waals interactions, and entropy.

The individual components of the determinations for binding free energy for interactions of the enzymes with clavulanate for the formation of the pre-acylation complexes are listed in Table 4. Comparison of the TEM-1  $\beta$ -lactamase and its M69L variant showed that the van der Waals energy is larger for the mutant by 1.7 kcal/mol. The electrostatic energy ( $\Delta E^{\text{elec}}$ ) decreased by 3.8 kcal/mol for the mutant enzyme but is offset by a 6.5 kcal/mol increase in the contribution of the electrostatic solvation free energy term to the total binding free energy ( $\Delta G^{\text{PB}}$ ). This leads to an overall unfavorable contribution of the electrostatic component for the M69L variant. No change was observed for the nonpolar contribution to the solvation free energy ( $\Delta G^{\text{SA}}$ ). This is not unexpected, given that the nonpolar contribution to the solvation energy is proportional to the solvent-accessible surface area of the protein, which does not change as a result of M69L mutation. The entropy change ( $-2.9$  kcal/mol) has a stabilizing effect on  $\Delta\Delta G_{\text{bind}}^{\text{calc}}$ . The favorable contribution of the entropy arises from a decrease in the motions in the side chain of the larger L69 residue. Overall, the change in the binding free energy as a result of mutation in M69L ( $\Delta\Delta G_{\text{bind}}^{\text{calc}}$ ) is unfavorable by  $1.4 \pm 0.6$  kcal/mol and agrees well with the free energy change of  $1.9 \pm 0.2$  kcal/mol measured experimentally from the dissociation constants. It would appear that the electrostatic component is an important part of this change in the binding free energy, along with the entropy and van der Waals components.

This finding is consistent with the crystallographic observation for the lack of binding of the sulfate anion to the mutant enzyme (Figure 2). The surface of the active site of the mutant variant could not support binding of the sulfate for the same reason that binding of the carboxylate group of clavulanate is impaired in the pre-acylation complex. It is the attenuated contribution to the binding free energy from the electrostatic energy component that accounts for both observations. The net energetic effect is small, and indeed the structural attributes leading to it cannot be visualized by inspection of the X-ray structures.

We find the selection of the M69L mutation in the TEM-1  $\beta$ -lactamase remarkable. As mutant enzymes go, this is seemingly a most insignificant change that nature can make in a

(51) Murcko, A. M. *J. Med. Chem.* **1995**, *38*, 4953.

(52) Böhm, H.-J.; Stahl, M. *Med. Chem. Res.* **1999**, *9*, 445.

(53) Tame, J. R. H. *J. Comput.-Aided Mol. Des.* **1999**, *13*, 99.

(54) Massova, I.; Kollman, P. A. *J. Am. Chem. Soc.* **1999**, *121*, 8133.



protein. The mutated site, amino acid 69, is not within the active site, and indeed the side chain of the amino acid at this position is directed away from the active site. The clinically observed M69L mutation did not cause any change in the local or global structure of the mutant enzyme compared to the wild-type, as discerned from analyses of the high-resolution X-ray structures for the two proteins. Accordingly, the kinetic parameters for turnover of typical antibiotic substrates for this enzyme have not been affected by the mutation; hence, the mutant variant is a fully functional resistance enzyme. The effect of the mutation is manifesting itself in a subtle way in the differential dynamics motion of the mutant variant compared to the wild-type enzyme in the general vicinity of the active site. The end result is a small difference of  $1.9 \pm 0.2$  kcal/mol ( $1.4 \pm 0.6$  kcal/mol by computation) on the binding energy for the formation of the noncovalent pre-acylation complex, as determined for clavulanate. This difference was found to be the result of an increase in the van der Waals and electrostatic components of the binding free energy. It is important to point out that when the formation of the pre-acylation complex is forced onto the mutant  $\beta$ -lactamase in *in vitro* experiments with purified enzyme, all the subsequent events depicted in Scheme 1 would appear to take place virtually unencumbered, as evidenced by the parameters of Table 2. It is noteworthy that the  $\Delta\Delta G_{\text{bind}}^{\text{exp}}$  values for the formation of the pre-acylation complex for sulbactam and tazobactam are  $2.0 \pm 0.3$  and  $2.9 \pm 0.3$  kcal/mol, respectively. The effect is the largest for tazobactam. But since the dissocia-

tion constant for tazobactam with the wild-type enzyme is 20 nM, the mutations brings the value of the dissociation constant to 2.6  $\mu$ M. Despite the largest kinetic effect seen for tazobactam, this inhibitor has the least affect with respect to the manifestation of the inhibitor-resistant phenotype.

It is likely that the M69L inhibitor-resistant  $\beta$ -lactamase was selected clinically in response to the use of the antibiotic mixtures that contained either clavulanate or sulbactam (based on the  $K_I$  values of Table 2). This mutant  $\beta$ -lactamase is remarkable in light of the mechanistic and structural subtleties that we discussed in the foregoing paragraph. But also it is a significant example of how nature would take the smallest incremental change on an existing template—the wild-type structure—to create an enzyme of expanded functional usefulness for the organism that harbors it. The change is small in every sense of the word, but it is sufficient for the expanded function. We have no doubt that there are other examples such as these in nature awaiting characterization.

**Acknowledgment.** Synchrotron facilities for data collections were provided by ESRF (beamline BM30) and DESY (X31). The work in France was funded in part by the Program de Recherche Fondamentale en Microbiologie (MENRT) and CNRS. The work in the United States was supported by a grant from the National Institutes of Health (S.M.).

JA026547Q